Investigation of the Dimensional Stability of ACQ-Treated Southern Pine When Supplemented with Wax and Different Types of Nano-SiO_2

Lili Yu,[a,*] Junwang Meng,[a] Zhenzhong Tang,[b] Lizhi Zhu,[a] Junyan Zhu,[a] and Xiaojun Ma [a]

Southern pine (*Pinus* spp.) wood cubes were treated with amine copper quaternary (ACQ) solutions supplemented with wax and different types of nano-SiO_2 particles. The effects of various types of nano-SiO_2 on the dimensional stability of ACQ-treated wood were investigated, including water absorption, swelling, and shrinkage. The results showed that nano-SiO_2/wax treatments improved the hydrophobicity of the ACQ-treated wood; various types of nano-SiO_2 particles had different effects on the water absorption by the wood. The best water absorption resistance was observed with the ACQ-treated wood modified with nano-SiO_2 that had a specific surface area of 380 m^2/g. However, the nano-SiO_2/wax treatment had a negligible effect on the swelling and shrinkage resistance of the ACQ-treated wood; various types of nano-SiO_2 did not affect the swelling and shrinkage of the wood.

Keywords: Amine copper quaternary (ACQ); Nano-SiO_2; Wax; Dimensional stability

*Contact information: a: Department of Wood Science and Technology, Tianjin University of Science and Technology, P. O. Box 546, Tianjin 300222, China; b: Timber Value Promotion and Substitution Administration Center, Beijing 100834, China; *Corresponding author: yulilucky@tust.edu.cn*

INTRODUCTION

The application of a water-borne preservative, such as alkaline copper quaternary (*i.e.*, a copper amine with a quaternary ammonium compound), to treat wood has become more and more widely employed. Such treated wood is used in construction, outdoor furniture, utensils, and children's playground sets; these applications require long service life, easy processing, good visual appearance, and good mechanical properties of the building material. However, water or moisture will be readily absorbed by the preservative-treated wood. This phenomenon is caused by the high hygroscopicity of constituents of wood (cellulose, hemicelluloses, and lignin), as well as the ingredients of the wood preservative, which lack hydrophobic constituents (Yu *et al.* 2011; Qing *et al.* 2017). The decay of preservative-treated wood structures can be avoided either by the exclusion of water or moisture or by introducing water repellents into the treated wood (Evans *et al.* 2009; Yu *et al.* 2016). Similarly, a protective coating, such as a stain (Nejad *et al.* 2012; Shah *et al.* 2017), can be used to protect wood from both moisture intrusion and from ultraviolet radiation attack.

In recent years, as part of the growing interest in nanotechnology, nanoparticles and the corresponding treatments have been widely applied to wood modification to enhance wood quality. The impregnation of the wood fiber walls with inorganic nanocompounds, such as silica (SiO_2), titanium dioxide (TiO_2), zinc oxide (ZnO), and others, improves the water repellency, photostability, flame retardancy, and mechanical properties of the treated material (Mahltig *et al.* 2008; Clausen *et al.* 2011; Kong *et al.* 2017). Among various

available nanoparticles, silica nanoparticles are more useful for the modification of treated wood due to their amorphous structure, high purity (more than 99% in most products), and high specific surface area (Bahadori and Hosseini 2012). Ślosarczyk (2017) showed that an important element of tailoring the properties of silica aerogel nanocomposite was the right choice of the type and the length of the carbon material. Shi *et al.* (2007) employed nano-SiO_2 to improve wood properties and discovered that the dimensional stability, hardness, and flame resistance of the treated samples were enhanced. Roumeli *et al.* (2012) reported that particleboards bonded with ureaformaldehyde (UF)/nano-SiO_2 led to increased water resistance of the resulting panels. Also, the addition of nano-silica has been shown to assist as a barrier to gas and moisture penetration into the treated wood; this has been proved by a strong decrease in water absorption (Sangermano *et al.* 2005). The variation in the size of nanoparticles and their hydrophobic character was investigated by varying the amount of precursor in the reaction system (Zulfiqar *et al.* 2016). Zulfiqar *et al.* (2017) indicated that the combination of hydrophobic silica nanoparticles and adhesive could protect the surfaces building materials from external damage without inducing a significant decrease in superhydrophobicity. Our previous work (Yu *et al.* 2017) reported increased dimensional stability when nano-SiO_2 particles and wax were applied to ACQ-treated wood.

The aim of the present work was to examine the effect of different types of nano-SiO_2 combined with wax on the dimensional stability of ACQ-treated wood. We employ various dimensional stability tests, which include water absorption, wood swelling, and wood shrinkage measurements. This research will provide results that will be useful for enhancing the performance of ACQ-treated wood for outdoor applications.

EXPERIMENTAL

Material and Methods

Samples

Sapwood of kiln-dried southern pine without any defects (*Pinus* spp.) was cut into small cubes with dimensions of 19.0 mm x 19.0 mm x 19.0 mm; the cubes were stored in a conditioning room (50 °C and 60% relative humidity) to obtain an equilibrium moisture content of 9 to 10%. The mass of the conditioned cubes was determined, and cubes with similar masses were selected. Eighteen replicates per treatment were used to perform the dimensional stability and contact angle tests.

Nano-SiO_2 water solution

Four different types of nano-SiO_2 particles where obtained from Zhejiang Hongsheng Material Technology Co., Ltd (China). These nano-SiO_2 particles where hydrophilic and had a 99.5% purity. The particles had an average size of 20 nm.

The BET specific surface areas of these four different types of nano-SiO_2 were 60, 150, 200, and 380 m^2/g, respectively. Because the nano-SiO_2 particles were insoluble in the water, trisodium phosphate was used to aid dissolution in the water solution; analytically pure trisodium phosphate was purchased from Tianjin Kemi Chemical Reagent Co., Ltd (China). The ratio of nano-SiO_2 to trisodium phosphate was set to 1:10 based on our previous work (Yu *et al.* 2016, 2017); 0.6, 0.8, 1.3, and 1.9 g of different types of nano-SiO_2 (BET of 60, 150, 200 and 380 m^2/g) and corresponding mass of trisodium phosphate were added into 100 g deionized water, respectively. The solutions were stirred using a

magnetic stirrer for 1 h and then subjected to ultrasonic processing at 40 °C for 30 min. If the solution was not clear, then the mixture solution was stirred using the magnetic stirrer again until the nano-SiO_2 and trisodium phosphate were completely dissolved.

ACQ/wax modification preservatives

The mass fraction of the active components (33.3% dodecyl dimethyl benzyl ammonium chloride and 66.7% copper oxide) in ACQ preservative is 15%. Two sets of ACQ solutions were used for impregnation. The first solution set contained 0.6% ACQ preservative, and the second set contained 0.6% ACQ preservative mixed with 2.5% paraffin wax to form an emulsion. The paraffin wax had a melting point between 58 and 60 °C and had a purity of 40%. Both the concentrations of ACQ and wax were the same concentrations used in the final formulation of the wood preservatives.

Sample vacuum-pressure impregnation treatment

Sample treatments were performed vacuum-pressure impregnation with different types of nano-SiO_2 water solutions and oven dried at 60 °C to achieve constant weight. Then the samples were vacuum-pressure impregnated with different ACQ or ACQ/wax modification solutions as shown in Table 1. The vacuum-pressure treatment was set as follows: The samples were put into the pressure chamber, and the vacuum was set to -0.1 MPa for 1 h to remove the air in the chamber and in the wood samples. The solution was admitted into the samples. The vacuum was released, and the pressure was elevated to 0.8 MPa for another 1 h to promote more solution permeating into the samples. Then the pressure was released and the samples were removed from the pressure chamber. The treated samples were post-treated at 70 °C for 10 h with hot air circulation to accelerate the fixation of ACQ treated wood and then oven dried at 60 °C to achieve constant weight. After drying, the dimensional stability tests were performed according to standard GB/T 1934 (2009).

Table 1. Experimental Treatment Conditions for Wood Samples

Experimental designation	Nano-SiO_2		ACQ concentration (%)	Wax concentration (%)
	BET specific surface area (m^2/g)	Maximum solubility (g/100g)		
T1	0	0		0
T2	60	0.6		2.5
T3	150	0.8		2.5
T4	200	1.3		2.5
T5	380	1.9		2.5

Dimensional Stability Test

Water absorption measurement

All the treated and untreated specimens were conditioned in an oven, which was set to 60 ± 2 °C, for 24 h; afterwards, the specimens were cooled over anhydrous cupric sulfate in a desiccator prior to testing. The water absorption measurements were performed

in accordance with Chinese Standard GB/T 1934.1 (2009) as described by Yu *et al*. (2016). The percent of water absorption (WA) by the samples was calculated according to Eq. 1,

$$WA = \frac{W_2 - W_1}{W_1} \times 100\% \quad (1)$$

where W_1 and W_2 are the masses of each specimen before and after the water absorption measurement.

Wood swelling measurement

Samples were conditioned during the moisture absorption measurements at 65 ± 3% relative humidity and 20 ± 2 °C until the dimensions stabilized. The wood swelling measurements were conducted in accordance with Chinese Standard GB/T 1934.2 (2009) as described by Yu *et al*. (2016). The percentages of the tangential and radial moisture absorption swelling (*MTS* and *MRS*) by the samples were calculated using Eqs. 2 and 3,

$$MTS = \frac{TS_2 - TS_1}{TS_1} \times 100\% \quad (2)$$

$$MRS = \frac{RS_2 - RS_1}{RS_1} \times 100\% \quad (3)$$

where TS_1 and TS_2 are the tangential dimensions of each specimen before and after the swelling measurement, respectively, and RS_1 and RS_3 are the radial dimensions of each specimen before and after the swelling measurement, respectively.

The percentages of the tangential and radial water absorption swelling (*WTS* and *WRS*) of the samples were determined by using Eqs. 4 and 5,

$$WTS = \frac{TS_3 - TS_1}{TS_1} \times 100\% \quad (4)$$

$$WRS = \frac{RS_3 - RS_1}{RS_1} \times 100\% \quad (5)$$

where TS_1 and TS_3 are the tangential dimensions of each specimen before and after the swelling measurement, respectively, and RS_1 and RS_3 are the radial dimensions of each specimen before and after the swelling measurement, respectively.

Wood shrinkage measurement

Treated and untreated specimens were immersed into deionized water at 20 ± 2 °C until the dimensions stabilized; afterwards, the soaked specimens were subjected to air drying or to oven drying shrinkage measurements. The wood shrinkage measurement was performed in accordance to Chinese Standard GB/T 1934.2 (2009) as described by Yu *et al*. (2016). The percentages of tangential and radial air drying shrinkage (*ATS* and *ARS*) by the samples were computed using Eqs. 6 and 7,

$$ATS = \frac{TL_1 - TL_2}{TL_1} \times 100\% \quad (6)$$

$$ARS = \frac{RL_1 - RL_2}{RL_1} \times 100\% \quad (7)$$

where TL_1 and TL_2 are the tangential dimensions of each specimen before and after the shrinkage measurement, respectively, and RL_1 and RL_2 are the radial dimensions of each specimen before and after the shrinkage measurement, respectively. The tangential and radial oven drying shrinkage (*OTS* and *ORS*) by the wood samples were computed using Eqs. 8 and 9,

$$OTS = \frac{TL_1 - TL_3}{TL_1} \times 100\% \quad (8)$$

$$ORS = \frac{RL_1 - RL_3}{RL_1} \times 100\% \quad (9)$$

where TL_1 and TL_3 are the tangential dimensions of each specimen before and after the shrinkage measurement, respectively, and RL_1 and RL_3 are the radial dimensions of each specimen before and after the shrinkage measurement, respectively.

Contact Angle Measurement

Contact angles of different types of nano-SiO_2 on the water absorption performance of the treated wood were measured at room conditions of 20 ℃ and 40% RH. The contact angles between water and wood specimen surfaces were determined using a sessile-drop system (First Ten Angstroms FTA200 equipped with CCD camera and image analysis software). This system uses video image processing, which allows faster determination of dynamic contact angles compared to the conventional contact angle goniometry. Six replicates in each test group were used to calculate the maximum contact angles of different treated wood.

RESULTS AND DISCUSSION

Water Absorption Analysis

Water absorption results (as a percentage) of the ACQ-treated wood with different nano-SiO_2 particles combined with wax are presented in Fig. 1. The water absorption test was carried out for approximately 16 d. As observed in Fig. 1, the curves of the various wood treatments had similar water absorption trends. In the early stage (0 to 1 d), the water permeated quickly into the voids of the wood, such as the intercellular spaces and the lumens of the fibers. In the late stage (1 to 16 d), all the water absorption rates of the treated wood samples were much slower, and the samples tended to reach a plateau value, which corresponded to the saturation state for the wood. During these two different stages, the ACQ-treated wood with wax and different types of nano-SiO_2 had better water resistance performance than the ACQ-treated wood alone (T1).

As can be observed from Fig. 1, the moisture content for the control (T1) was approximately 130%, while the other treatments had moisture contents of approximately 100%, except for T5 (380 m^2/g nano-SiO_2 modified), which had a moisture content of approximately 90%. The soaking time to reach the maximum moisture content was much longer for T1 (control) than the other treatments in the early stage. This observation is

likely attributable to the hydrophobic wax with the nano-SiO_2 particles of the T2 to T5 treatments, which repelled the moisture intrusion into the samples. In the late stage, the rate of water absorption in the ACQ-treated wood (T1) was much faster than in other nano-SiO_2/wax treated wood (T2 to T5). For the final saturation moisture content, it was as high as 160% for the T1 treatment, while it was much lower for T2 to T5 treatments; the lowest saturation moisture content was observed for the T5 treatment (380 m^2/g nano-SiO_2 modified), which was only approximately 100%. These results demonstrated that the nano-SiO_2 particles combined with wax effectively decreased the hygroscopicity of the ACQ-treated wood. Moreover, the effects of various types of nano-SiO_2 particles on the water absorption resistance of treated wood differed considerably. Among the four types of nano-SiO_2 particles, the particles that had a BET specific surface area of 380 m^2/g had the highest water absorption resistance, which was also proved by the results of contact angles as shown in Table 2. These results demonstrated that silica nanoparticles with the higher surface area have better water absorption resistance. It could be due to the fact that silica nanoparticles with higher surface area create more rough surface texture as compared to other nanoparticles with the lower surface area. When coupled with the nonpolar character of wax, the rough surface morphology formed by silica nanoparticles could lead to better hydrophobic properties.

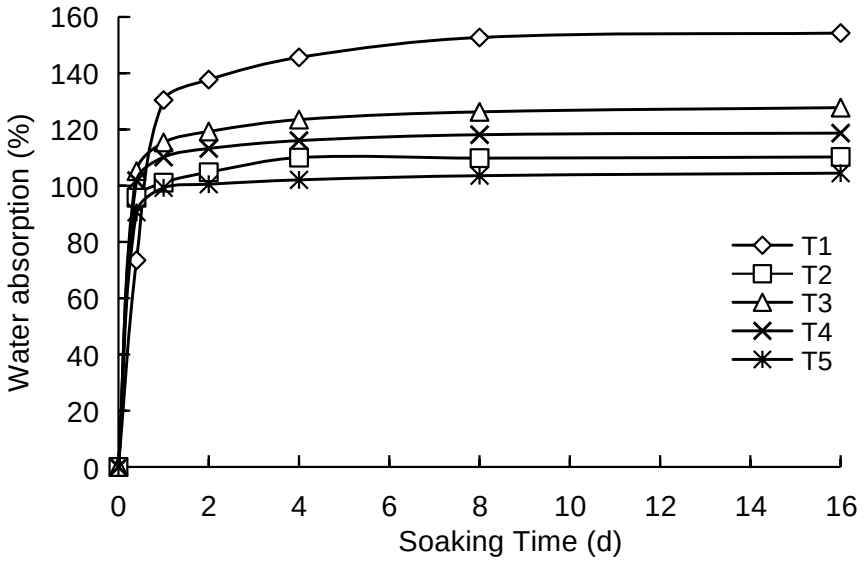

Fig. 1. Water absorption of ACQ-treated wood with different nano-SiO_2/wax treatments

Table 2. Maximum Contact Angles of ACQ-treated Wood with Different nano-SiO2/wax Treatments

Experiment	T1	T2	T3	T4	T5
Contact Angle (°)	64	128	106	119	134

Swelling Analysis

Tangential and radial swelling results (as a percentage) for the ACQ-treated wood during air drying with different nano-SiO_2/wax treatments are presented in Fig. 2. During

air drying period, the moisture content in the treated wood was turned from oven drying state to air drying state.

As shown in this period, the moisture was adsorbed quickly into wood in the initial 1 d, and then the rates of moisture adsorption began to slow down and reach the air drying moisture content after 8 d test. As observed in Fig. 2a, the radial swelling for T1 (ACQ-treated only) was approximately 1%, whereas it was a little higher, 2% to 3%, for T2 to T5 (ACQ-treated with nano-SiO_2/wax). Various types of nano-SiO_2 particles had different effects on the radial swelling. The 60 m^2/g nano-SiO_2 (T2) had the lowest swelling resistance (*i.e.*, the highest swelling), whereas the higher specific surface area nano-SiO_2 particles had similar swelling resistance levels. Somewhat similar trends were also observed with the tangential swelling results (Fig. 2b). The best swelling resistance was observed with the ACQ-treated wood modified with 380 m^2/g nano-SiO_2 combined with wax (T5).

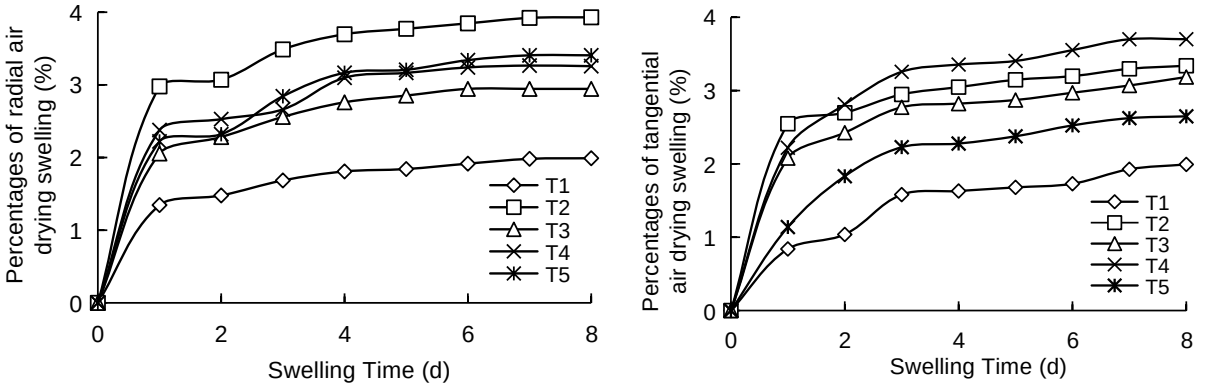

(a) Radial air drying swelling (b) Tangential air drying swelling

Fig. 2. Swelling of ACQ-treated wood during air drying with various nano-SiO_2/wax treatments

Tangential and radial swelling results (as a percentage) for ACQ-treated wood with various nano-SiO_2/wax treatments during oven drying are presented in Fig. 3. During oven drying period, the moisture content in the treated wood was turned from an oven drying state to a water saturation stage. As shown in this period, the percentages of radial swelling in the treated wood increased quickly in the initial 20 d, which corresponded to the moisture content from near 0 to moisture saturation point, and then the rates of radial swelling began to achieve the saturation state after 30 d water absorption test.

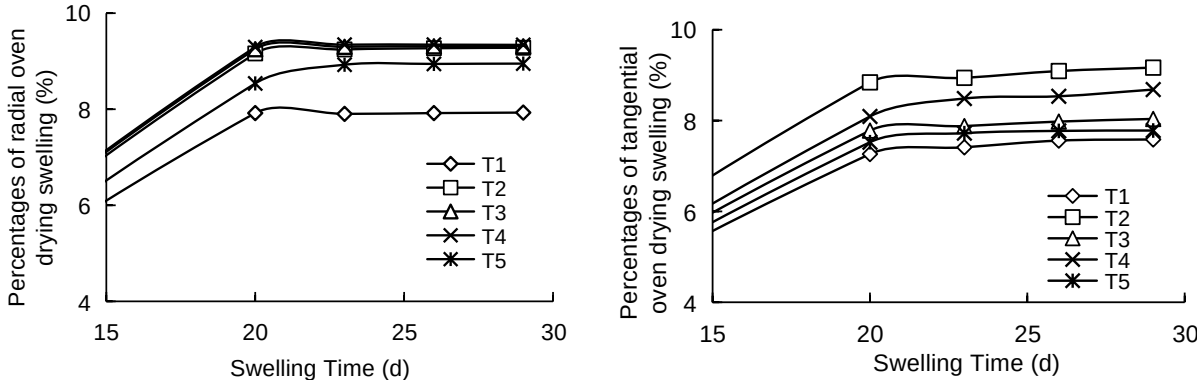

(a) Radial oven drying swelling (b) Tangential oven drying swelling

Fig. 3. Swelling of ACQ-treated wood during oven drying with various nano-SiO_2/wax treatments

As can be observed from Fig. 3, compared to T1 (ACQ-treated only), the rates of radial and tangential swelling in the other groups were a little higher, although the difference was also only 1 to 2%, especially for the rates of tangential swelling in T5 group (380 m^2/g nano-SiO_2 modified), which was very near to T1. Various types of nano-SiO_2 particles had different effects on swelling; the best swelling resistance was observed with the ACQ-treated wood that had 380 m^2/g nano-SiO_2/wax (T5).

Shrinkage Analysis

Tangential and radial air drying shrinkage results (as a percentage) for ACQ-treated wood with various nano-SiO_2/wax treatments are presented in Fig. 4. During the air drying period, the moisture content in the treated wood was turned from a water saturation state to an air drying stage. As shown in this period, the percentages of the radial and tangential shrinkage increased quickly in the initial 3 d, which corresponded to the moisture content from moisture saturation point to near air drying moisture content, and then the rates of water shrinkage began to slow down and reach the air drying state after the 8 d test. As observed from Fig. 4a, compared to T1 (ACQ-treated only), the rates of radial shrinkage in the other treated wood with wax and different types of nano-SiO_2 modification were a little higher, although the difference was only about 2%. Moreover, it was observed that the different types of nano-SiO_2 had little influence on the radial shrinkage; all four types of nano-SiO_2/wax (T2 to T5) had nearly identical results. Similar trends were observed for the tangential shrinkage (Fig. 4b).

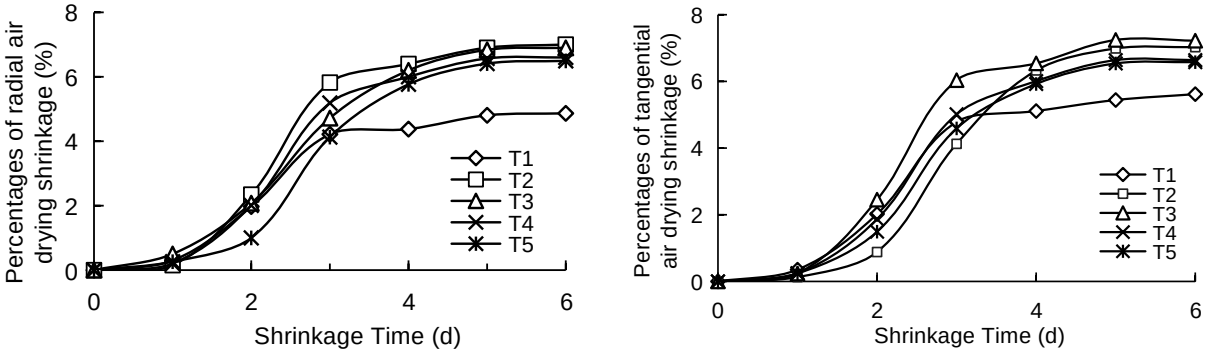

(a) Radial air drying shrinkage (b) Tangential air drying shrinkage

Fig. 4. Shrinkage of ACQ-treated wood during air drying with various nano-SiO_2/wax treatments

Tangential and radial oven drying shrinkage results (as a percentage) for ACQ-treated wood with various nano-SiO_2/wax treatments are presented in Fig. 5. During oven drying period, the moisture content in the treated wood was turned from a water saturation state to an oven drying state. As shown in this period, the radial and tangential shrinkage increased quickly in the initial 3 d, which corresponded to the moisture content from moisture saturation point to near 0, and then the rates of water shrinkage began to achieve the saturation state. As can be observed from Fig. 5a, compared to T1 (ACQ-treated only), the rates of radial shrinkage in the other treated wood with wax and different types of nano-SiO_2 modification were also a little higher, and the difference was about 2%. Similar trends were observed for the tangential shrinkage as showed in Fig. 5b. Various types of nano-SiO_2 had little effect on the radial shrinkage, whereas the type of nano-SiO_2 had an obvious effect on the tangential shrinkage.

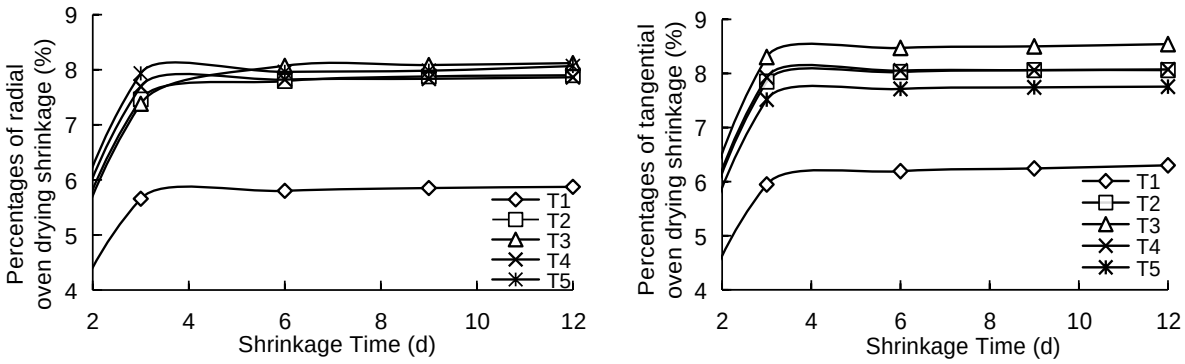

(a) Radial oven drying shrinkage (b) Tangential oven drying shrinkage

Fig. 5. Shrinkage of ACQ-treated wood during oven drying with various nano-SiO_2/wax treatments

CONCLUSIONS

1. During the water absorption process, ACQ-treated wood that was modified with different types of nano-SiO_2 combined with wax (T2 to T5) had better water resistance than the ACQ-treated only wood (T1). This observation demonstrated that nano-SiO_2 combined with wax improved the hydrophobicity of the ACQ-treated wood. The effects of various nano-SiO_2 particles with different specific surface areas on water absorption were noticeable, and the ACQ-treated wood modified with 380 m^2/g nano-SiO_2/wax (T5) had the best water absorption resistance. This observation was attributed to this nano-SiO_2 having the highest solubility in the preservative solution.
2. For the tangential and radial swelling of the ACQ-treated wood during air and oven drying, the swelling rates with nano-SiO_2/wax treated wood (T2 to T5) were a little higher than those of the ACQ-treated wood alone (T1). Various types of nano-SiO_2 had little effect on the swelling. Similar results were also observed from the tangential and radial shrinkage of ACQ-treated wood during air and oven drying. Treatment with nano-SiO_2/wax had little effect on the swelling and shrinkage resistance of the ACQ-treated wood.

ACKNOWLEDGMENTS

The authors are grateful for the financial support of the Subjects of National Natural Science Foundation of China (NSFC No. 31400499), the Student Laboratory Innovation Fund Project for Tianjin University of Science and Technology (1606A213), and the National College Students Innovation and Entrepreneurship Training Program (201610057018).

REFERENCES CITED

Bahadori, H., and Hosseini, P. (2012). "Reduction of cement consumption by the aid of silica nano-particles (investigation on concrete properties)," *J. Civil Eng. Manag*. 18(3), 416-425. DOI: 10.3846/13923730.2012.698912

Clausen, C. A., Kartal, S. N., Arango, R. A., and Green III, F. (2011). "The role of particle size of particulate nano-zinc oxide wood preservatives on termite mortality and leach resistance," *Nanoscale Res. Lett.* 6, 427. DOI: 10.1186/1556-276X-6-465

Evans, P. D., Wingate, H. R., and Cunningham, R. B. (2009). "Wax and oil emulsion additives: How effective are they at improving the performance of preservative-treated wood," *For. Prod. J.* 59(1-2), 66-70.

GB/T1934.1 (2009). "Method for determination of the water absorption of wood," Standardization Administration of China, Beijing, China.

GB/T 1934.2 (2009). "Method for determination of the swelling of wood," Standardization Administration of China, Beijing, China.

GB/T 1932 (2009). "Standard method for determination of the shrinkage of wood," Standardization Administration of China, Beijing, China.

Kong, L., Tu, K., Guan, H., and Wang, X. (2017). "Growth of high-density ZnO nanorods on wood with enhanced photostability, flame retardancy and water repellency," *Appl. Surf. Sci.* 407, 479-484. DOI: 10.1016/j.apsusc.2017.02.252.

Mahltig, B., Swaboda, C., Roessler, A., and Böttcher, H. (2008). "Functionalising wood by nanosol application," *J. Mater. Chem.* 18(27), 3180-3192. DOI: 10.1039/B718903F

Nejad, M., Ung, T., and Cooper, P. (2012). "Effect of coatings on ACQ preservative component distribution and solubility after natural weathering exposure," *Wood Sci. Technol.* 46(6), 1169-1180. DOI: 10.1007/s00226-012-0472-0

Qing, Y., Liu, M., Wu, Y., Jia, S., Wang, S., and Li, X. (2017). "Investigation on stability and moisture absorption of superhydrophobic wood under alternating humidity and temperature conditions," *Results Phys.* 7, 1705-1711. DOI: 10.1016/j.rinp.2017.05.002

Roumeli, E., Papadopoulou, E., Pavlidou, E., Vourlias, G., Bikiaris, D., Paraskevopoulos, K., and Chrissafis, K. (2012). "Synthesis, characterization and thermal analysis of ureaformaldehyde/nano SiO_2 resins," *Thermochim. Acta* 527, 33-39. DOI: 10.1016/j.tca.2011.10.007

Sangermano, M., Malucelli, G., Amerio, E., Priola, A., Billi, E., and Rizza, G. (2005). "Photopolymerization of epoxy coatings containing silica nanoparticles," *Prog. Org. Coat.* 54(2), 134-138. DOI: 10.1016/j.porgcoat.2005.05.004

Shah, M., Zulfiqar, U., Hussain, S. Z., Ahmad, I., Rehman, H., Hussain, I., and Subhani, T. (2017). "A durable superhydrophobic coating for the protection of wood materials," *Mater. Lett.* 203, 17-20. DOI:10.1016/j.matlet.2017.05.126

Shi, J., Li, J., Zhou, W., and Zhang, D. (2007). "Improvement of wood properties by urea-formaldehyde resin and nano-SiO_2," *Front. For. China* 2(1), 104-109. DOI: 10.1007/s11461-007-0017-0

Ślosarczyk, A. (2017). "Synthesis and characterization of silica aerogel-based nanocomposites with carbon fibers and carbon nanotubes in hybrid system," *Journal of Sol-Gel Science and Technology* 83, 912-920. DOI: 10.1007/s10971-017-4470-4

Yu, L., Cao, J., and Gao, W. (2011). "Evaluation of ACQ-D treated Chinese fir and Mongolian Scots pine with different post-treatments after 20 months of exposure," *Int. Biodeter. Biodegr*. 65(4), 585-590. DOI: 10.1016/j.ibiod.2011.03.001

Yu, L., Tang, Z., Wei, D., Zhu, L., Zhu, J., and Ma, X. (2016). "Evaluation of the dimensional stability and leaching performance of ACQ/wax treated southern pine," *BioResources* 11(4), 10201-10212. DOI: 10.15376/biores.11.4.10201-10212

Yu, L., Cai, J., Wang, Y., Liu, D., Tang, Z., and Zhu, J. (2017). "Improved dimensional stability of nano-SiO_2/wax modified ACQ treated southern pine," *BioResources* 12(4), 7515-7524.

Zulfiqar, U., Hussain, S., Awais, M., Mohsin, M., Khana, J.,Hussainb, I., Husaina, S., and Subhani, T. (2016). "In-situ synthesis of bi-modal hydrophobic silica nanoparticles for oil-water separation," *Colloids and Surfaces A: Physicochem. Eng. Aspects* 508, 301-308. DOI: 10.1016/j.colsurfa.2016.08.07

Zulfiqar, U., Awais, M., Hussain, S.Z., Hussainb, I., Hussain, S., and Subhani, T. (2017). "Durable and self-healing superhydrophobic surfaces for building materials," *Materials Letters* 192, 56-59. DOI: 10.1016/j.matlet.2017.01.070

Article submitted: June 20, 2017; Peer review completed: August 26, 2017; Revised version received and accepted: September 22, 2017; Published: October 2, 2017.
DOI: 10.15376/biores.12.4.8672-8682